

EFFECT OF MAGNETIC FIELD ON BLOOD FLOW THROUGH AN ARTERY: A NUMERICAL MODEL

J. C. MISRA, G. C. SHIT

Centre for Theoretical Studies

Indian Institute of Technology, Kharagpur, India

e-mail: jcm@maths.iitkgp.ernet.in, gopal_iitkgp@yahoo.co.in

В этой статье мы исследовали нестационарное течение крови, рассматривая ее несжимаемой ньютоновской проводящей жидкостью в прямом сегменте эластичной артерии под воздействием однородного поперечного магнитного поля. Проблема решалась численно в приближении модели локального течения. Были исследованы эффекты синусоидального изменения формы стенки и пульсирующего градиента давления. Для анализа течения использовалась неявная схема. Реологические параметры крови, доступные из научной литературы, были использованы для моделирования различных участков кровеносной системы. Графически представлено влияние эффектов движения стенок и магнитного поля на профиль скорости и натяжение стенок сосудов, а также на расход крови от времени. Было показано, что скорость движения крови и натяжение стенок уменьшаются с усилением магнитного поля. Исследование представляет интерес для врачей, поскольку влияние внешнего магнитного поля может контролировать течение крови. Результаты могут быть полезны для лечения болезней артерий типа артериальной гипертензии.

Introduction

Recently, the study of blood flow through arteries has gained serious attention of researchers, physiologists and clinical persons because blood and blood vessels are substantial health risk factors and can substantially contribute to morbidity and mortality. Blood flow in the human circulatory system depends upon the pumping action of the heart which in turn produces a pressure gradient throughout the system. The rheological properties of blood and the motion of the arterial wall play an important role in the physiology of the cardiovascular system.

It is well known that at high shear-rates blood behaves like a Newtonian fluid during flows through large blood vessels (cf. Misra et al. [2] and Copley [3]). But in particular situations blood may behave as a non-Newtonian fluid, even in large arteries, as reported in [4–6]. It is also worthwhile to mention here that although blood is non-Newtonian suspension of cells in plasma, MacDonald [7] remarked that for vessels of radius greater than 0.025 cm, blood may be considered as a homogeneous Newtonian fluid. Several studies [8–10] of

physiological fluid dynamics through stenosed arteries have been carried out to evaluate the flow pattern and the shear stress at the walls under steady and pulsatile conditions by considering blood as a Newtonian fluid. Pontrelli [11] studied the steady axisymmetric flow of blood in a constricted rigid tube. Dutta et al. [1] investigated numerically the oscillatory and pulsatile flows of Newtonian fluids in straight elastic tubes with the assumptions of Ling and Atabek's [12] local flow model. They presented a theoretical assesment of the local flow model and the range of validity of the assumption. Again Dutta et al. [13] investigated the possible effects of non-Newtonian behaviour of blood on flow through an elastic artery. Rodkiewicz et al. [14] studied the behaviour of blood flow in arteries under steady and pulsatile conditions using both the Newtonian and non-Newtonian model as suggested by Walburn and Schneck [15]. Shyy and Sun [16] gave the numerical solution of a steady viscous flow in fixed-wall vessels for a variety of non-uniformities on the channel wall.

Since blood consists of a suspension of red blood cells containing hemoglobin which contains iron oxide, it is quite apparent that blood is electrically conducting and exhibits magnetohydrodynamic flow characteristics. It may, however, be pointed out that proteins like hemoglobin are extremely complex molecules which are sensitive to seemingly minor changes in pH and composition of blood. For example, the deoxy-configuration of hemoglobin is the state in which oxygen binds the heme group; a slight decrease in pH (for instance from 7.4 to 7.2) reduces the affinity of oxygen for hemoglobin (the Bohr effect) with various consequences for the absorption from and release of oxygen to living cells and tissues. Many authors [17–19] have investigated the flow of blood through arteries in the presence of magnetic field under different conditions. In fact the Lorentz force arising out of the flow across the magnetic lines of force acts on the constituent particles of blood and alters the hemodynamic indicators of blood flow. The potential use of such MHD principles in prevention and rational therapy of arterial hypertension was explored by Vardanyan [20], who showed that for steady flow of blood in an artery of circular cross-section, a uniform transverse magnetic field alters the flow rate of blood. Recently Misra et al. [21, 22] investigated the steady MHD flow of a viscous fluid in a slowly varying channel in the presence of a uniform magnetic field.

In the present study we investigated the influence of magnetic field on blood flow through an artery, the wall of which is elastic. The study pertains to a situation where a magnetic field is applied in a direction transverse to the direction of flow. Such a field has a more pronounced effect on the flow than that in the case of an axial magnetic field. Of specific interest is to determine the velocity profile, the variation of wall shear stress and the flow rate with time at different radial phase angles and unsteadiness parameters. The hemodynamic effects for various blood vessels having different diameters, like aorta, femoral artery, carotid artery and coronary artery.

1. Formulation of the Problem and the Theoretical Analysis

Let us consider the flow of blood in a straight circular cylindrical section of an artery, by treating blood as a viscous homogeneous incompressible fluid. We use cylindrical polar coordinates (r^*, θ^*, z^*) , with z^* as the central axis of the artery. Due to symmetry, the flow variation is independent of θ^* . Denoting by u^*, v^* the velocity components of blood along the axial and radial directions respectively, the equations of motion governing the flow of

blood in the presence of a transverse magnetic field may then be put in the form

$$\frac{\partial u^*}{\partial t^*} + u^* \frac{\partial u^*}{\partial z^*} + v^* \frac{\partial u^*}{\partial r^*} = -\frac{1}{\rho} \frac{\partial p^*}{\partial z^*} + \nu \left(\frac{\partial^2 u^*}{\partial r^{*2}} + \frac{1}{r^*} \frac{\partial u^*}{\partial r^*} + \frac{\partial^2 u^*}{\partial z^{*2}} \right) - \frac{\sigma B_0^2}{\rho} u^* \quad (1)$$

and

$$\frac{\partial v^*}{\partial t^*} + u^* \frac{\partial v^*}{\partial z^*} + v^* \frac{\partial v^*}{\partial r^*} = -\frac{1}{\rho} \frac{\partial p^*}{\partial r^*} + \nu \left(\frac{\partial^2 v^*}{\partial r^{*2}} + \frac{1}{r^*} \frac{\partial v^*}{\partial r^*} - \frac{v^*}{r^{*2}} + \frac{\partial^2 v^*}{\partial z^{*2}} \right), \quad (2)$$

while the equation of continuity is

$$\frac{\partial u^*}{\partial z^*} + \frac{\partial v^*}{\partial r^*} + \frac{v^*}{r^*} = 0 \quad (3)$$

in which ν is the kinematic viscosity and ρ the density of blood, p^* the fluid pressure, σ the electrical conductivity and B_0 the applied magnetic field. The induced magnetic field produced by the motion of the blood in the presence of the external magnetic field is assumed negligible.

We consider axisymmetry of flow, and simplify the equations of motion by using the long-wave-length approximation $\left| \frac{\omega R}{c} \right| \ll 1$, ω being the angular frequency, R the radius and c the wave speed. Then the axial viscous transport terms are negligible, so that the radial equation of motion simply reduces to $\frac{\partial p^*}{\partial r^*} = 0$ and the axial equation of motion assumes the form

$$\frac{\partial u^*}{\partial t^*} + u^* \frac{\partial u^*}{\partial z^*} + v^* \frac{\partial u^*}{\partial r^*} = -\frac{1}{\rho} \frac{\partial p^*}{\partial z^*} + \nu \left(\frac{\partial^2 u^*}{\partial r^{*2}} + \frac{1}{r^*} \frac{\partial u^*}{\partial r^*} \right) - \frac{\sigma B_0^2}{\rho} u^*. \quad (4)$$

Introducing non-dimensional variables,

$$z = \frac{z^*}{R_0}, \quad r = \frac{r^*}{R_0}, \quad u = \frac{u^*}{U}, \quad v = \frac{v^*}{U}, \quad p = \frac{p^*}{\rho U^2}, \quad t = \frac{t^* U}{R_0} \quad (5)$$

the equations (4) and (3) can be written as

$$\frac{\partial u}{\partial t} + u \frac{\partial u}{\partial z} + v \frac{\partial u}{\partial r} = -\frac{\partial p}{\partial z} + \frac{1}{\text{Re}} \left(\frac{\partial^2 u}{\partial r^2} + \frac{1}{r} \frac{\partial u}{\partial r} \right) - \frac{M^2}{\text{Re}} u \quad (6)$$

and

$$\frac{\partial u}{\partial z} + \frac{\partial v}{\partial r} + \frac{v}{r} = 0 \quad (7)$$

where $\text{Re} = \frac{UR_0}{\nu}$ is the Reynolds number and $M = B_0 R_0 \sqrt{\frac{\sigma}{\rho \nu}}$ the Magnetic parameter (Hartman number).

In order to specify our problem, it is necessary to prescribe the local tube wall motion $R(t^*)$ and the pulsatile pressure gradient $\frac{\partial p}{\partial z}(t^*)$, which determines the nature of the flow. We take

$$R(t^*) = \bar{R}[1 + k_r \sin(\omega t^* + \phi)] \quad (8)$$

and

$$-\frac{\partial p}{\partial z}(t^*) = \bar{K} + k_p \cos(\omega t^*) \quad (9)$$

where \bar{R} is the mean radius of the artery, \bar{K} the mean pressure gradient, k_r , k_p are amplitude parameters and ϕ the phase angle along with the frequency ω .

The boundary conditions for the present problem are assumed as

$$\frac{\partial u}{\partial r} = 0, \quad v = 0 \quad \text{at } r = 0, \quad (10)$$

$$u = 0, \quad v = \frac{\partial R}{\partial t} \quad \text{at } r = R(t, z). \quad (11)$$

The problem is difficult to solve due to the moving boundary condition (11).

Let us use the coordinate transformation

$$\xi = \frac{r}{R(t, z)}. \quad (12)$$

The local flow model [1] does not require axial boundary condition because it takes care of the following assumption due to Ling and Atabek [12]:

$$\frac{\partial u}{\partial z} = f(z, t)|u| \quad (13)$$

where $f(z, t)$ is an unknown function which can be determined from the radial velocity boundary condition (11). Neglecting the natural taper of an artery, which is in general small (cf. Milnor [23]) the transformed governing equation (6) reads

$$\frac{\partial u}{\partial t} = -\frac{\partial p}{\partial z} + \frac{1}{\text{Re}R^2} \left(\frac{\partial^2 u}{\partial \xi^2} + \frac{1}{\xi} \frac{\partial u}{\partial \xi} \right) + \left(\frac{\xi}{R} \frac{\partial R}{\partial t} - \frac{v}{R} \right) \frac{\partial u}{\partial \xi} + \frac{u}{R} \left(\frac{\partial v}{\partial \xi} + \frac{v}{\xi} \right) - \frac{M^2}{\text{Re}} u. \quad (14)$$

Let us write the derivative $\frac{\partial R}{\partial z}$ as $\frac{\partial R}{\partial z} = \frac{\partial R}{\partial p} \frac{\partial p}{\partial z}$, where $\frac{\partial R}{\partial p}$ describes the elastic response of the artery, whose experimental values are available in [24]. Also using the transformation (12), the equation (7) becomes

$$\frac{\partial u}{\partial z} + \frac{1}{R} \frac{\partial v}{\partial \xi} + \frac{v}{\xi R} - \frac{\xi}{R} \frac{\partial R}{\partial z} \frac{\partial v}{\partial \xi} = 0. \quad (15)$$

Multiplying equation (15) by ξR , then integrating it with respect to ξ and using the boundary condition (11), we get

$$v = \frac{\partial R}{\partial p} \frac{\partial p}{\partial z} \left[\xi u - \frac{2}{\xi} \left(\int_0^\xi \xi u d\xi - \frac{\int_0^1 \xi u d\xi}{\int_0^1 \xi |u| d\xi} \int_0^\xi \xi |u| d\xi \right) \right] + \frac{1}{\xi} \frac{\partial R}{\partial t} \frac{\int_0^\xi \xi |u| d\xi}{\int_0^1 \xi |u| d\xi}. \quad (16)$$

Also the boundary conditions are transformed to

$$\frac{\partial u}{\partial \xi} = 0, \quad v = 0 \quad \text{at } \xi = 0, \quad (17)$$

$$u = 0, \quad v = \frac{\partial R}{\partial t} \quad \text{at } \xi = 1. \quad (18)$$

In terms of the non-dimensional variables defined in (5), the equation (8) and (9) can be rewritten as

$$R(t) = \bar{R} \left[1 + k_r \sin \left(\frac{\alpha^2 t}{\text{Re}} + \phi \right) \right] \quad (19)$$

and

$$-\frac{\partial p}{\partial z}(t) = \bar{K} + k_p \cos \left(\frac{\alpha^2 t}{\text{Re}} \right) \quad (20)$$

where $\alpha = R_0 \sqrt{\frac{\omega}{\nu}}$ is the unsteadiness parameter (Womersley number).

After having determined the velocity components of blood in different arteries, we can obtain the volumetric flow rate Q and the wall shear stress τ_w from the relations

$$Q(t) = 2\pi \int_0^R r u(r, t) dr = 2\pi R^2 \int_0^R \xi u(\xi, t) d\xi \quad (21)$$

and

$$\tau_w = -\mu \frac{\partial u}{\partial r} \Big|_{r=R} = -\frac{\mu}{R} \frac{\partial u}{\partial \xi} \Big|_{\xi=1}. \quad (22)$$

2. Numerical Method

The transformed governing equations (14) and (16) subject to the boundary conditions (17) and (18) are solved numerically using the finite difference implicit Crank-Nicolson scheme. The central differences are employed to discretize the derivatives along the ξ -direction and forward differences are used along the t -direction. The index for time appears as superscript and the index for space direction as in the subscript to locate the grid points. n denotes time instant t and $(n+1)$ time instant $(t+\delta t)$. The following discretization is used in equation (14)

$$\frac{\partial^2 u}{\partial \xi^2} = \frac{1}{2} \left(\frac{u_{i+1}^{n+1} - 2u_i^{n+1} + u_{i-1}^{n+1}}{\partial \xi^2} + \frac{u_{i+1}^n - 2u_i^n + u_{i-1}^n}{\partial \xi^2} \right) + O((\delta \xi)^2), \quad (23)$$

$$\frac{\partial u}{\partial \xi} = \frac{1}{2} \left(\frac{u_{i+1}^{n+1} - u_{i-1}^{n+1}}{2\partial \xi} + \frac{u_{i+1}^n - u_{i-1}^n}{2\partial \xi} \right) + O((\delta \xi)^2), \quad (24)$$

$$\frac{\partial v}{\partial \xi} = \frac{v_{i+1}^n - v_{i-1}^n}{2\partial \xi} + O((\delta \xi)^2), \quad (25)$$

$$\frac{\partial R}{\partial t} = \frac{R(t^{n+1}) - R(t^n)}{\partial t} + O(\delta t). \quad (26)$$

Using the equations (23)–(26), (14) can be rewritten as

$$(-r_1 + r_2)u_{i-1}^{n+1} + (1 + 2r_1)u_i^{n+1} + (-r_1 - r_2)u_{i+1}^{n+1} = D_i^n, \quad i = 0, 1, 2, 3, \dots, m \quad (27)$$

where

$$r_1 = \frac{\delta t}{2\text{Re}R^2\partial \xi^2}, \quad (28)$$

$$r_2 = \frac{\delta t}{4R\delta \xi} \left(\xi_i \frac{\partial R}{\partial t} - v_i^n \right), \quad (29)$$

$$r_3 = \frac{\delta t}{2R\xi_i\partial\xi} u_i^n \{ \xi_i(v_{i+1}^n - v_{i-1}^n) + 2\delta\xi v_i^n \} \quad (30)$$

and

$$D_i^n = -\delta t \frac{\partial p}{\partial z} + r_1(u_{i+1}^n - 2u_i^n + u_{i-1}^n) + r_2(u_{i+1}^n - u_{i-1}^n) + r_3 + \left(1 - \frac{M^2\delta t}{\text{Re}}\right) u_i^n \quad (31)$$

with $\xi_i = i\delta\xi$, $i = 0, 1, 2, 3, \dots, m$ and $t^n = n\delta t$, $n = 0, 1, 2, 3, \dots$

For each time step, the system of linear equations (27) is expressed as a tri-diagonal system of equations which are then solved by using Thomas algorithm to compute the axial velocity. Using the axial velocity, the radial velocity can be computed explicitly from the equation

$$v_i^{n+1} = \frac{\partial R}{\partial p} \frac{\partial p}{\partial z} \left[\xi_i u_i^{n+1} - \frac{2}{\xi_i} \left(\int_0^{\xi_i} \xi_i u_i^{n+1} d\xi - \frac{\int_0^1 \xi_i u_i^{n+1} d\xi}{\int_0^1 \xi_i |u_i^{n+1}| d\xi} \int_0^{\xi_i} \xi_i |u_i^{n+1}| d\xi \right) \right] + \frac{1}{\xi_i} \frac{\partial R}{\partial t} \frac{\int_0^{\xi_i} \xi_i |u_i^{n+1}| d\xi}{\int_0^1 \xi_i |u_i^{n+1}| d\xi}. \quad (32)$$

The cardiac cycle T is divided into 100 equal time steps, by taking $\delta t = 0.01$ and the normalized inner radius ξ is divided into 40 equal spaces, with $\delta\xi = 0.025$. All numerical integrations are carried out using Simpson's three-eighths rule. The sinusoidal flow simulations are started from rest (zero velocity).

3. Results and Discussion

The objective of the present work has been to investigate the behaviour of blood flow through elastic arteries in the presence of an external magnetic field under the action of pulsatile pressure gradient, when the arterial wall motion is sinusoidal. With the end in view, in order to illustrate the applicability of the theoretical analysis, a numerical approach has been developed and computational work has been carried out by using experimental data for different physiological parameters available in the existing literatures [1, 7, 23–27]. In the numerical scheme, the step sizes in the ξ - and t -directions have been taken to be $\delta\xi = 0.025$ and $\delta t = 0.01$ respectively. It has been seen that further reduction in the values of $\delta\xi$ and δt does not bring about any change in the computed values before 4th or 5th decimal places. Necessary numerical data for computation, like the mean radius of various arteries, mean pressure gradient and the amplitude of the pressure are presented in Table 1. In the sinusoidal flow simulations, k_r has been set at 0.05 which corresponds to 5 percent radius variation over a cardiac cycle, this is a typical value for arteries [7].

The pressure amplitude k_p has been taken to be 20% of mean pressure gradient \bar{K} . We have considered the values of the unsteady parameter $\alpha = 3, 4, 6, 12$, the magnetic parameter $M = 0, 2, 4, 6$, the radius phase angle $\phi = 0, \frac{\pi}{4}, \frac{2\pi}{3}, \pi$ and $\mu = 0.035P$. In physiological flow simulation $M = 0$ corresponds to normal flow of blood, in the absence of any magnetic field.

Таблица 1. Necessary numerical data for computation

Blood vessels	Radius (\bar{R}), cm	\bar{K} , dyne/cm ³	k_p , dyne/cm ³
Aorta	1.0	7.3	1.46
Femoral artery	0.5	32.0	6.4
Carotid artery	0.4	50.0	10.0
Coronary artery	0.15	698.65	139.73

Таблица 2. Comparison of axial velocity profiles in coronary artery

$\xi = r/R$	Present results	Results of Chaturani et al.(1990)
0.0	98.53	98.12
0.2	95.01	95.10
0.4	83.69	84.11
0.6	63.95	64.84
0.8	36.01	36.93

In the absence of any magnetic field, Table 2 gives a comparison between the velocity profile in coronary artery and that reported by Chaturani et al. [25] who considered blood as a Casson fluid. Figure 1 gives a comparison of the results of the present study without magnetic field effect with those presented by Chakravarty et al. [28] who also treated blood as a Newtonian fluid.

Basing upon the computational results, qualitative and quantitative variation of axial velocity profiles in various parts of the circulatory system, with different parameters is presented in Figs. 2–8. Figs. 2–4 illustrate the extent to which the magnetic field intensity

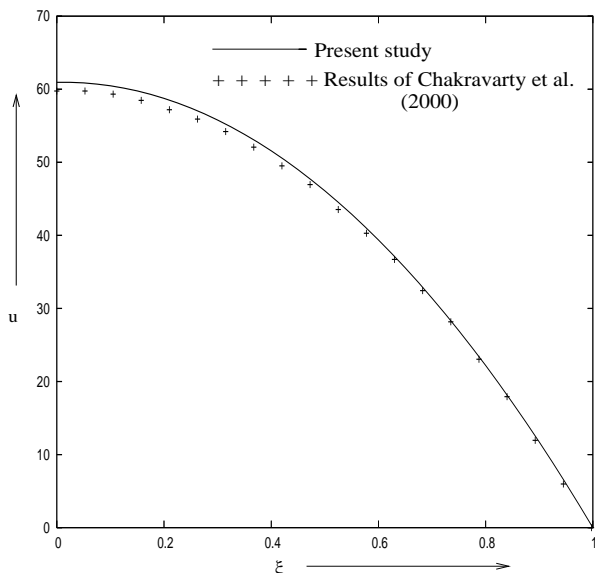


Fig. 1. Comparison of velocity profile in a coronary artery with: $\alpha = 4$, $\phi = 0$, $Re = 90$, $t = 0.25$, $\bar{K} = 50$ dyne/cm³, $M = 0$ (in the absence of any external magnetic field)

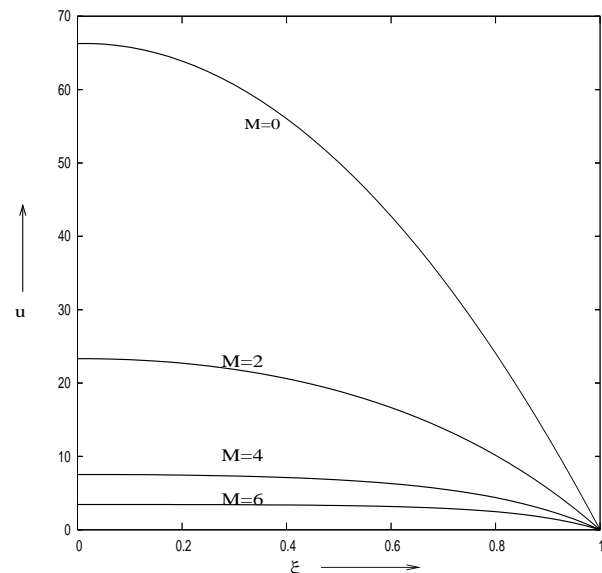


Fig. 2. Velocity profile in an aorta for different M with: $\alpha = 4$, $\phi = 0$, $Re = 15$, $t = 0.75$, $\bar{K} = 7.3$ dyne/cm³

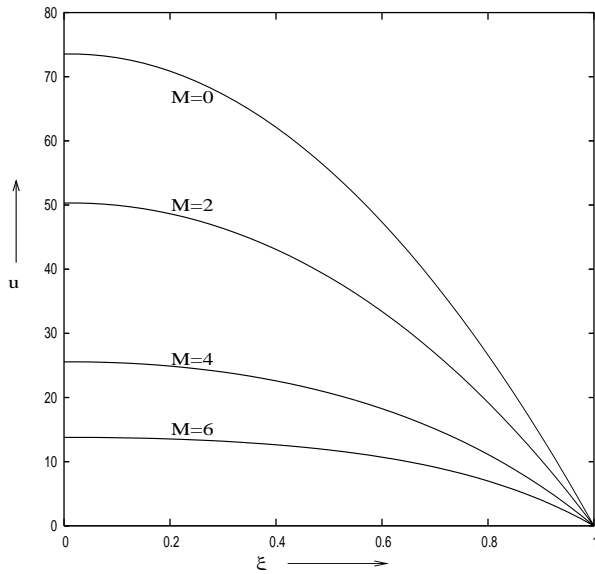


Fig. 3. Velocity profile in a femoral artery for different M with: $\alpha = 4$, $\phi = 0$, $Re = 15$, $t = 0.75$, $\bar{K} = 32$ dyne/cm³

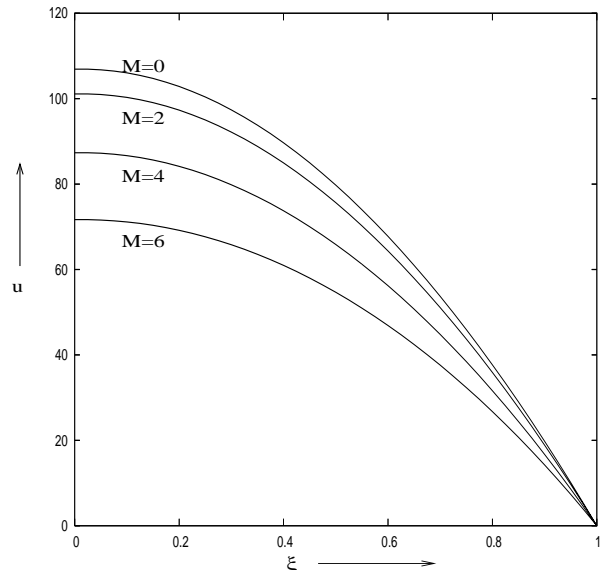


Fig. 4. Velocity profile in a coronary artery for different M with: $\alpha = 4$, $\phi = 0$, $Re = 10$, $t = 0.75$, $\bar{K} = 698.65$ dyne/cm³

can affect blood flow through different arteries (aorta, femoral artery, and coronary artery), by using experimental data presented in Table 1. It is of interest to note from these figures while in the case of large arteries the magnetic field intensity brings about greater changes in the axial velocity of blood, the changes are relatively small in the case of arteries of smaller dimensions. In each case, blood velocity decreases with the increase in magnetic field strength. These figures further show that for any given magnetic field strength the velocity is maximum along the central line of the artery and it gradually decreases along the radial direction and reduces to zero at the wall of the artery. One may further observe that in the case of aorta and femoral arteries, when the magnetic field strength is increased from zero to 2, the velocity drop in the central region is much greater than that in the case of coronary arteries. The scenario in the case of coronary arteries is, however, quite different. The magnitude of velocity drop with the increase in magnetic strength is found to increase for these arteries.

Figure 5 gives the variation of blood velocity with phase angle. The computational results indicate that velocity change in the case of aorta, is negligibly small. When ϕ increases from 0 to $\frac{\pi}{2}$, the velocity increases. But for $\frac{\pi}{2} < \phi < \pi$, the velocity decreases gradually with a slow rate with the increase in ϕ .

Plots for the velocity profile computed by using the respective experimental data for the pressure gradient given in Table 1, presented in Fig. 6 for the four different types of arteries studied here show that velocity is least for aorta and largest for coronary arteries. Figure 7 indicates that for a given pressure gradient, velocity in the aorta is the greatest and that in a coronary artery is the least. This implies, in order that at a specific radial distance the velocity in coronary artery is the same as that in aorta, a much larger mean pressure gradient will be necessary.

Figure 8 shows that up to a certain value of the unsteadiness parameter α , the central line velocity in an elastic artery maintains a constant value, beyond which it is of oscillatory

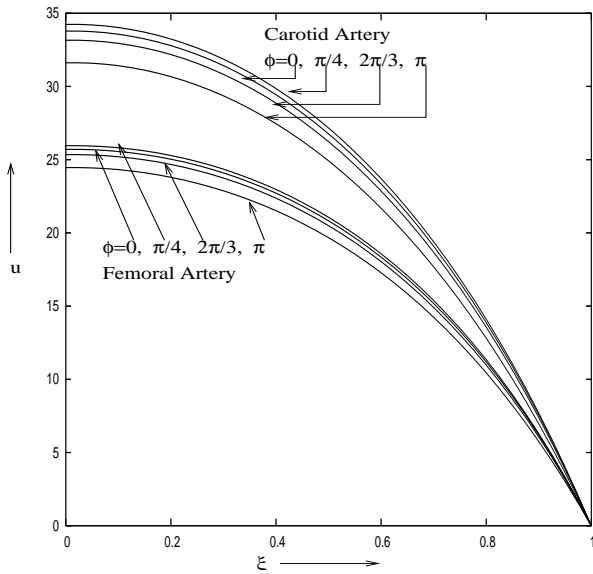


Fig. 5. Axial velocity profiles in femoral and carotid arteries for different phase angle with: $\alpha = 3, M = 4, Re = 15, t = 1.25$

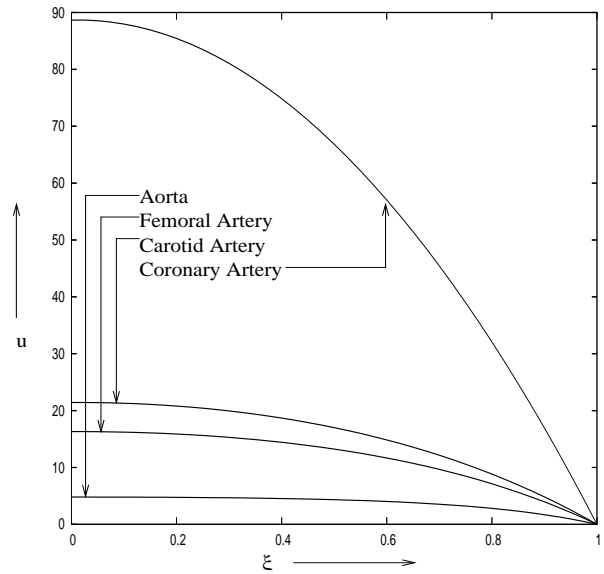


Fig. 6. Axial velocity profile in different arteries with: $\alpha = 3, \phi = 0, Re = 10, M = 4, t = 1.25$

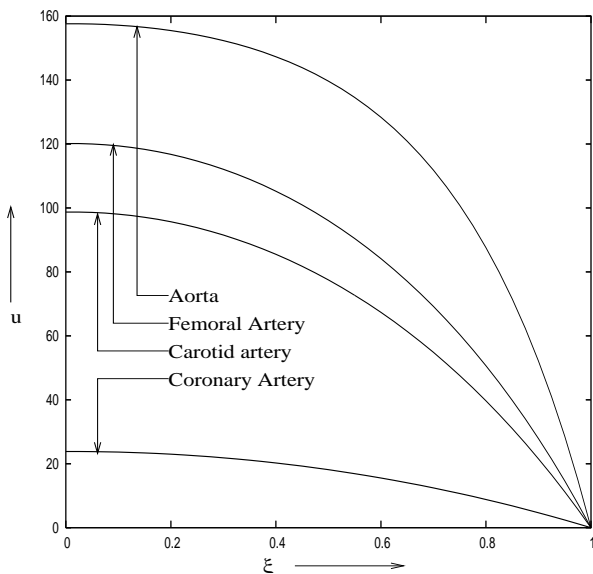


Fig. 7. Variation of axial velocity profile in different arteries under the same pressure amplitude with: $\alpha = 3, \phi = 0, Re = 50, M = 4, \bar{K} = 40.5 \text{ dyne/cm}^3, t = 1.25$

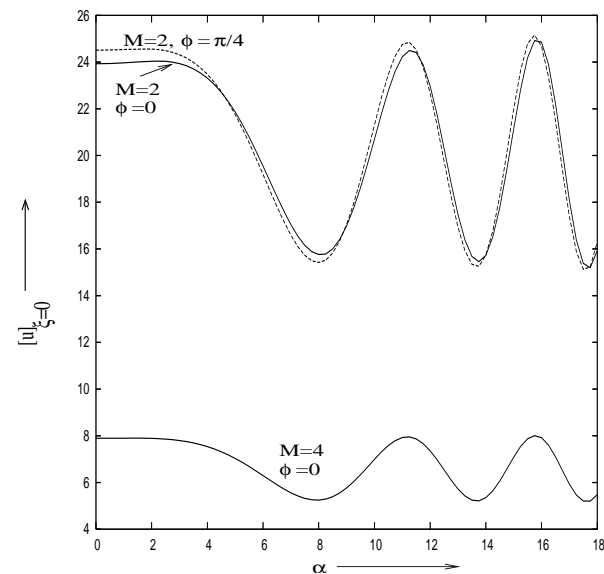


Fig. 8. Variation of center line velocity in an aorta with unsteadiness parameter for different M and radius phase angle with: $Re = 15, t = 0.75$

character. The time variation of the radial motion of the arterial wall in four different types of arteries is shown in Fig. 9, where computation has been carried out by taking the respective experimental data for the pressure gradient. It is seen that the radial velocity of the wall becomes negative in the systolic phase, while it is positive during diastole. Thus there occurs back flow near the arterial wall, causing separation in the flow field. This indicates that

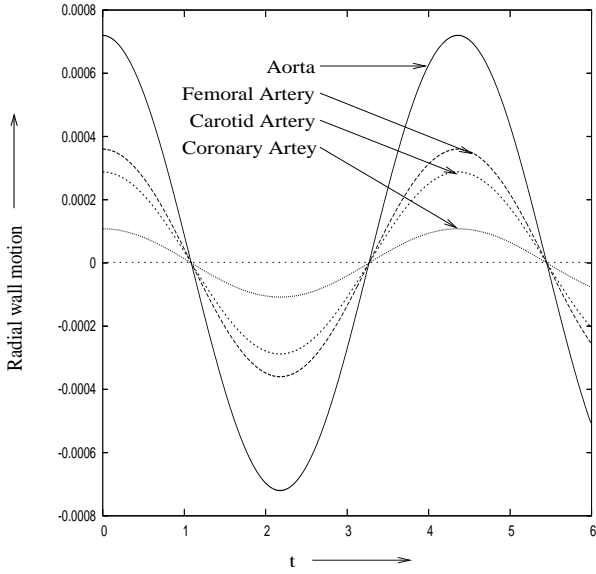


Fig. 9. Variation of radial velocity profile in different types of arteries with: $\alpha = 3$, $\phi = 0$, $Re = 50$, $M = 4$, $\bar{K} = 40.5 \text{ dyne/cm}^3$, $t = 1.25$

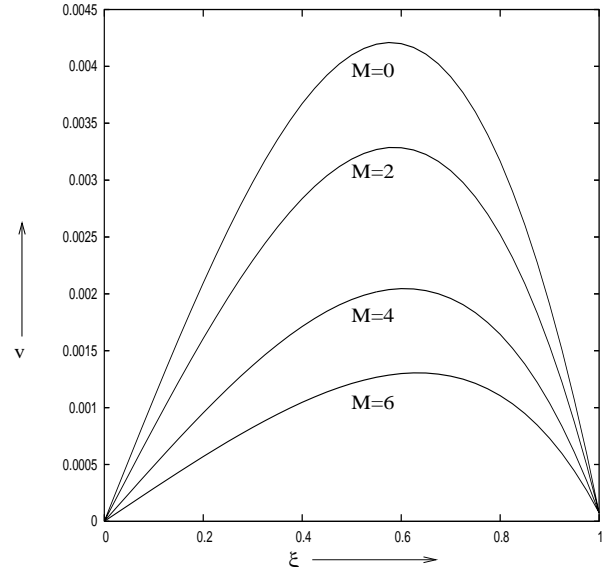


Fig. 10. Variation of radial velocity profile in a carotid artery for different M with: $\alpha = 3$, $\phi = 0$, $Re = 20$, $t = 1.25$

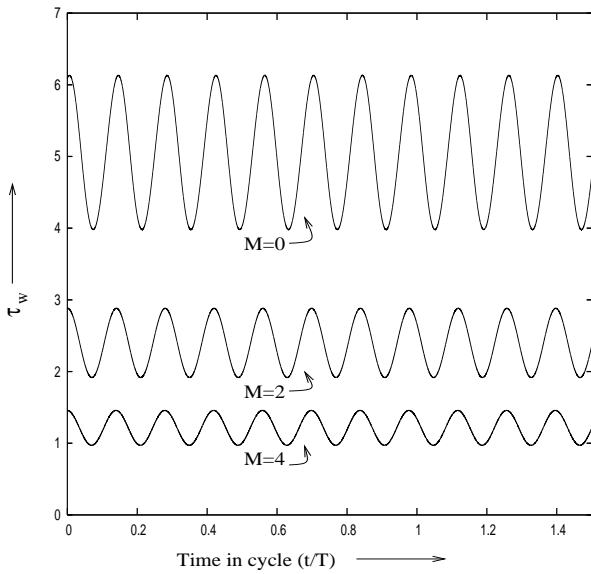


Fig. 11. Variation of wall shear stress with time in an aorta for different M with: $\alpha = 3$, $\phi = 0$, $Re = 20$

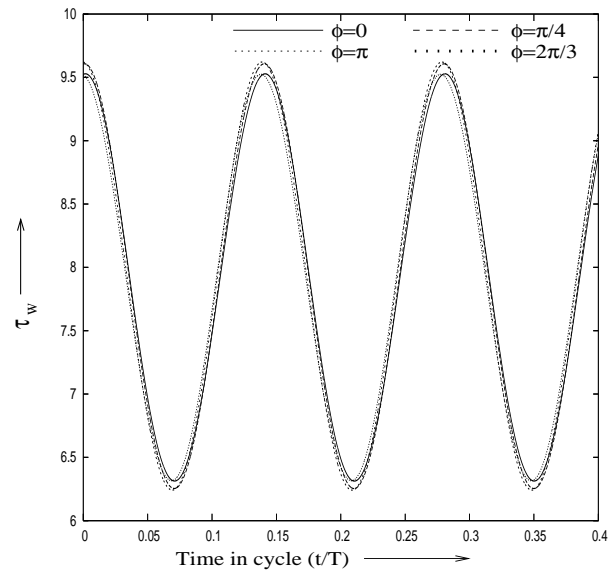


Fig. 12. Variation of wall shear stress with time in a carotid artery under different phase angle with: $\alpha = 3$, $M = 4$, $Re = 20$

the radial wall motion should affect the radial velocity more significantly than the axial velocity. It is also revealed that radial velocity of the arterial wall vanishes twice in each of the two cardiac cycles. Figure 10 depicts the variation of radial velocity of the arterial wall at $t = 1.25$. One can observe that the radial velocity decreases with the increase in magnetic field strength.

Figures 11–13 present the variation of wall shear stress with time in cycle for different types of arteries, different values of the magnetic parameter and different radius phase angles. It is seen from Fig. 12 that the wall shear stress reduces with the increase in the value of the magnetic parameter M . Figure 11 shows that for a given pressure gradient, the shear stress is maximum in aorta and minimum in coronary arteries. In all the cases under consideration

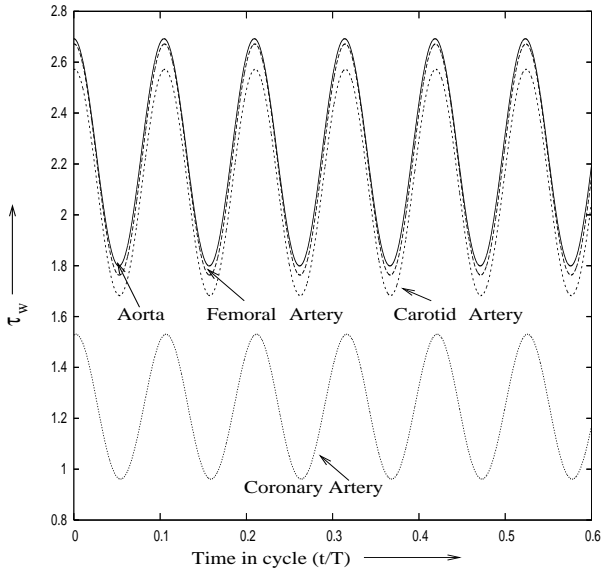


Fig. 13. Variation of wall shear stress with time in different arteries under the same pressure amplitude with: $\alpha = 3$, $\phi = \pi/4$, $M = 4$, $Re = 15$

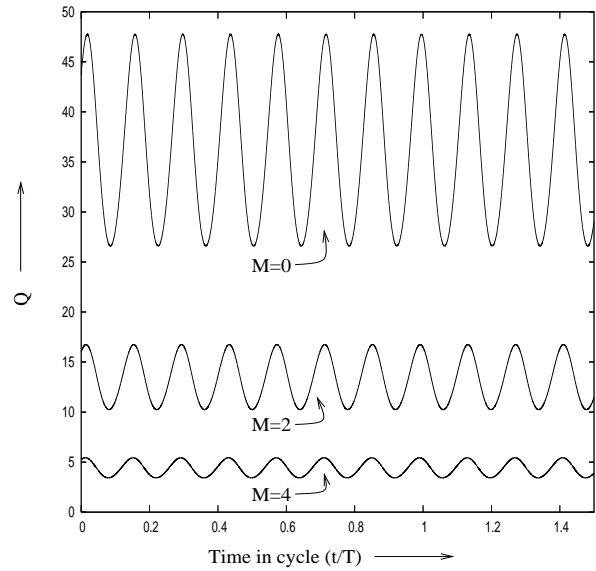


Fig. 14. Variation of the volumetric flow rate with time in an aorta for different M , when $\alpha = 3$, $\phi = 0$, $Re = 20$

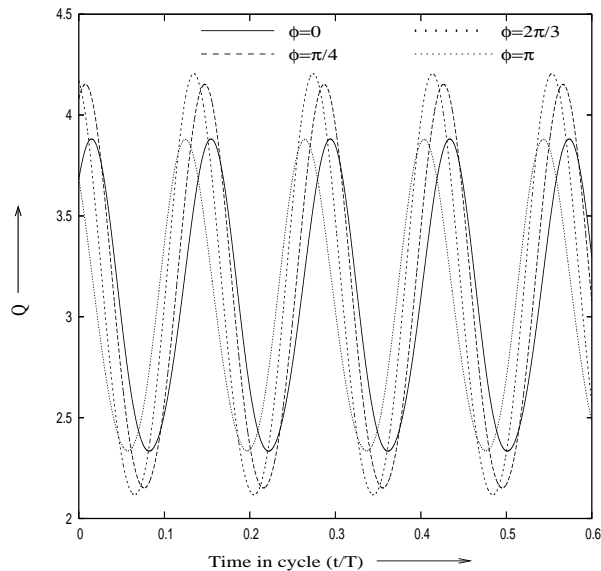


Fig. 15. Variation of volumetric flow rate in a carotid artery for different phase angles with: $\alpha = 3$, $M = 4$, $Re = 20$

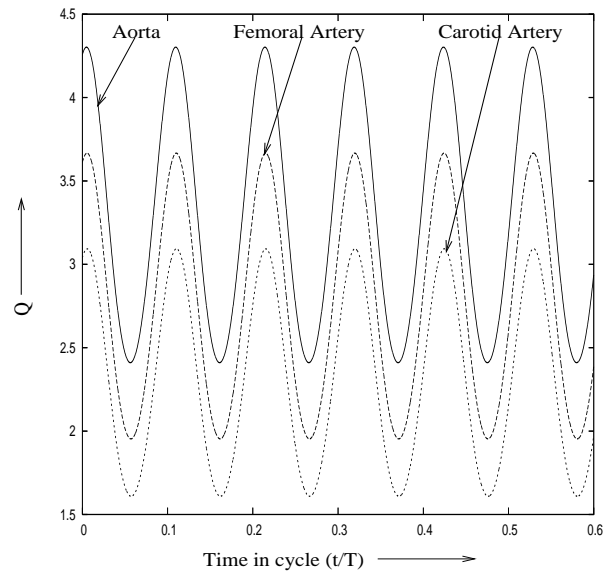


Fig. 16. Variation of volumetric flow rate with time in different arteries having different pressure amplitudes with: $\alpha = 3$, $\phi = \pi/4$, $M = 4$, $Re = 15$

the wall shear stress is found to oscillate with time. Such a behaviour is believed to owe its origin to the pulsatile pressure gradient produced by the heart.

Variation of flow rate Q with time in cycle, for an aorta with different values of the magnetic parameter M is shown in Fig. 14. It can be observed from this figure that the flow rate diminishes as M increases. For a fixed value of the magnetic parameter, the variation of flow rate with time in cycle for different phase angles is depicted in Fig. 15. It reveals that the volumetric flow rate for elastic arteries may increase or reduce considerably depending upon the radius phase angle, although the wall shear stress is not significantly affected by a change in the radius phase angle (cf. Fig. 13), as discussed earlier. Figure 16 gives the flow variation with time for aorta, femoral artery and carotid artery for given radius phase angle and magnetic parameter. This figure establishes the fact that the volumetric flow rate of blood increases with increase in the radius of arteries. It may also be observed that the flow rate of blood varies periodically with time.

Concluding Remarks

In the present theoretical study, an attempt has been made to examine various aspects of blood flow in different segments of the circulatory system in a situation where the system has been subjected to an external magnetic field. The elastic response of the arteries of various sizes has also been duly accounted for.

The governing equations are transformed by using radial coordinate transformation and using the considerations for local flow model. The detailed illustration of flow characteristics has been made numerically to perform some graphical presentation of the computed results. The study shows that the instantaneous flow characteristics are significantly affected by the magnetic parameter and unsteadiness parameter as well as by the radius phase angle. It reveals further that a magnetic field bears the potential to reduce the flow of blood through arteries, wall shear stress and the volumetric flow rate.

On the basis of the results presented here, it can be concluded that the flow of blood and pressure can be controlled sufficiently by the application of an external magnetic field. It is also possible to bring down these quantities to any desirable level by increasing/diminution of the magnetic field strength. Thus this investigation throws sufficient light towards the therapeutic use of the application of external magnetic field in the clinical treatment of hemodynamic diseases, like hypertension.

Acknowledgement: *The authors wish to express their sense of deep gratitude to the reviewer for kindly going through the manuscript carefully and for his esteemed comments appreciating highly the contents of the paper which he describes as an “intriguing” one and for pointing out that it bears potential application in the treatment of arterial diseases, like hypertension. One of the authors (J.C. Misra) is also thankful to the Council of Scientific and Industrial Research, New Delhi for supporting this investigation.*

References

- [1] DUTTA A., WANG D.M., TARBELL J.M. Numerical analysis of flow in an elastic artery model // J. Biomech. Engg. 1992. Vol. 114. P. 26–33.

- [2] MISRA J.C., CHAKRAVARTY S. Flow in arteries in the presence of stenosis // *J. Biomech.* 1986. Vol. 19. P. 907–918.
- [3] COPLEY A.L. Fluid mechanics and rheology // *Biorheology.* 1990. Vol. 27. P. 3–19.
- [4] NAKAMURA M., SAWADA T. Numerical study on flow of non-Newtonian fluid through axisymmetric stenosis // *J. Biomech. Engg.* 1988. Vol. 110. P. 247–262.
- [5] MURATA T. Theory of non-Newtonian viscosity of red cell deformation // *Biorheology.* 1983. Vol. 20. P. 471–483.
- [6] LIEPSCH D.W. Flow in tubes and arteries- A comparison // *Biorheology.* 1986. Vol. 23. P. 395–433.
- [7] McDONALD D.A. *Blood flow in arteries.* 2nd ed., London: Edward Arnold Publishers, 1974.
- [8] TU C., DEVILLE M., DHEUR L., VANDERCHUREN L. Finite element simulation of pulsatile flow through arterial stenosis // *J. Biomech.* 1992. Vol. 25. P. 1141–1152.
- [9] MISRA J.C., KAR B.K. Momentum integral method for studying flow characteristics of blood through a stenosed vessel // *Biorheology.* 1989. Vol. 26. P. 23–25.
- [10] PEDLEY T.J. *The fluid mechanics of large blood vessels.* Cambridge University Press, 1980.
- [11] PONTRELLI G. Blood flow through an axisymmetric stenosis // *Proc. Inst. Mech. Eng., J. Eng. in Medicine.* 2001. Vol. 215. P. 1–10.
- [12] LING S.C., ATABEK H.B. A non-linear analysis of pulsatile flow in arteries // *J. Fluid Mech.* 1972. Vol. 55. P. 493–511.
- [13] DUTTA A., TARBELL J.M. Influence of non-Newtonian behaviour of blood on flow in an elastic artery model // *J. Biomech. Engg.* 1996. Vol. 118. P. 111–119.
- [14] RODKIEWICZ C.M., SINHA P., KENNEDY J.S. On the application of a constitutive equation for whole human blood // *J. Biomech. Engg.* 1990. Vol. 112. P. 198–206.
- [15] WALBURN F.J., SCHNECK D.J. A constitutive equation for whole human blood // *Biorheology.* 1976. Vol. 13. P. 201.
- [16] SHYY W., SUN C.S. Development of a pressure correction/ staggered-grid based multigrid solver for incompressible recirculating flows // *Comput. Fluids.* 1993. Vol. 22. P. 51–76.
- [17] MISRA J.C., PAL B., GUPTA A.S. Hydromagnetic flow of a second-grade fluid in a channel — Some application to physiological systems // *Math. Models and Methods in Appl. Sci.* 1998. Vol. 8. P. 1323–1342.
- [18] MIDYA C., LAYEK G.C., GUPTA A.S., RAY MAHAPATRA T. Magnetohydrodynamic viscous flow separation in a channel with constrictions // *J. Fluids Engg.* 2003. Vol. 125. P. 952–962.
- [19] PAVLOV K.B. Magnetohydrodynamic flow of an incompressible viscous fluid caused by deformation of a plane surface // *Magnitnaya Gidrodinamika.* 1974. Vol. 4. P. 146–147.
- [20] VARDANYAN V.A. Effect of magnetic field on blood flow // *Biofizika.* 1973. Vol. 18. P. 491–496.

- [21] MISRA J.C., PAL B., GUPTA A.S. Oscillatory entry flow in a plane channel with pulsating walls // *Int. J. Non-Linear Mechanics*. 2001. Vol. 36. P. 731–741.
- [22] MISRA J.C., PAL B., GUPTA A.S. Steady hydrodynamic flow in a slowly varying channel // *Proc. National Acad. Sci., India*. 1996. Vol. 66(A). P. 247–262.
- [23] MILNOR W.R. *Hemodynamics*. 2nd ed., Baltimore: Williams and Wilkins, 1989.
- [24] GREENFIELD J.C., PATEL D.J. Relation between pressure and diameter in the ascending aorta of man // *Circ. Res.* 1962. Vol. 10. P. 778.
- [25] CHATURANI P., PALANISAMY V. Casson fluid model for pulsatile flow of blood under period body acceleration // *Biorheology*. 1990. Vol. 27. P. 619–630.
- [26] MISRA J.C., PAL B. A mathematical model for the study of the pulsatile flow of blood under an externally imposed body acceleration // *Math. Comp. Modelling*. 1999. Vol. 29. P. 89–106.
- [27] CRACIUNESCU O.I., CLEGG S.T. Pulsatile blood flow effects on temperature distribution and heat transfer in rigid vessels // *J. Biomech. Engg.* 2001. Vol. 123. P. 500–505.
- [28] CHAKRAVARTY S., MANDAL P.K. Two-dimensional blood flow through tapered arteries under stenotic conditions // *Int. J. Non-Linear Mechanics* 2000. Vol. 35. P. 779–793.

Received for publication 27 October 2006